

The Effect of Weak Lensing on the Angular Correlation Function of Faint Galaxies

R. Moessner, B. Jain and J. V. Villumsen

*Max Planck Institut für Astrophysik
Karl Schwarzschild-Str. 1,
85740 Garching, Germany*

4 September 2021

ABSTRACT

The angular correlation function $\omega(\theta)$ of faint galaxies is affected both by nonlinear gravitational evolution and by magnification bias due to gravitational lensing. We compute the resulting $\omega(\theta)$ for different cosmological models and show how its shape and redshift evolution depend on Ω and Λ . For galaxies at redshift greater than 1 (R magnitude fainter than about 24), magnification bias can significantly enhance or suppress $\omega(\theta)$, depending on the slope of the number-magnitude relation. We show for example how it changes the ratio of $\omega(\theta)$ for two galaxy samples with different number-count slopes.

Key words: galaxies: clustering - cosmology: observations - gravitational lensing - large scale structure of the Universe

1 INTRODUCTION

The angular correlation function of galaxies has been used to characterize the large-scale distribution of galaxies for over 2 decades. If the number density on the sky at angular position $\hat{\psi}$ is $n(\hat{\psi})$, then $\omega(\theta)$ is defined as

$$\omega(\theta) = \frac{\langle n(\hat{\psi})n(\hat{\phi}) \rangle}{\bar{n}^2} - 1. \quad (1)$$

The 3-dimensional unit vectors $\hat{\psi}$ and $\hat{\phi}$ are used to define the angular separation θ as $\hat{\psi} \cdot \hat{\phi} = \cos(\theta)$, and \bar{n} is the mean galaxy number density on the sky. The observed galaxy distribution is well described by a power law $\omega(\theta) \propto \theta^{-\gamma}$, with slope $\gamma \simeq 0.8$. Since $\omega(\theta)$ is a projection on the sky of the 3-dimensional auto-correlation function $\xi(r, z)$, the above power law for $\omega(\theta)$ has been associated with a power law for ξ with slope 1.8 which is close to the observed value in the nearby galaxy distribution. Measurements of $\omega(\theta)$ are difficult to interpret as it involves a projection of the galaxy distribution out to redshifts of order 1 (e.g. for a sample with limiting R magnitude of about 24.5). Thus the effects of evolution of large scale structure due to gravitational clustering as well as galaxy evolution need to be understood to interpret $\omega(\theta)$.

Recently Villumsen (1996) has considered the effect on $\omega(\theta)$ of gravitational lensing by large-scale structure along the line of sight (Gunn 1967). Lensing increases the area of a given patch on the sky, thus diluting the number density. On

the other hand, galaxies too faint to be included in a sample of given limiting magnitude are brightened due to lensing and may therefore be included in the sample. The net effect, known as magnification bias, can go either way: it can lead to an enhancement or suppression of the observed number density of galaxies, depending on the slope of the number-magnitude relation. Variations in the number density which are correlated over some angular separation alter $\omega(\theta)$. Villumsen (1996) showed how the linear evolution of density fluctuations along the line of sight can be used to compute the change in $\omega(\theta)$ due to magnification bias. The deflections of neighbouring photon trajectories due to lensing by large scale structure are very small, hence the calculation can be done in the limit of weak lensing.

In this paper we compute $\omega(\theta)$ for different cosmological models taking into account the effects of nonlinear gravitational evolution and gravitational lensing. Since $\omega(\theta)$ is a 2-point statistic, even in the fully nonlinear regime it is determined completely by the 3-dimensional power spectrum. We use extensions of the proposal of Hamilton et al. (1991) to include the nonlinear evolution of the power spectrum into the calculation of $\omega(\theta)$. We also include the dependence on the cosmological parameters Ω_m and Ω_Λ .

In Section 2 the formalism for computing $\omega(\theta)$ is presented. Section 2.1 discusses the effects of the cosmological model via the growth of density perturbations and the distance-redshift relation. Results for CDM-like power spectra for different values of Ω_m and Ω_Λ are presented in Sec-

tion 3. We explore ways to isolate the effect of the lensing contribution to $\omega(\theta)$ in Section 4 and conclude in Section 5.

2 THE EFFECT OF MAGNIFICATION BIAS ON THE ANGULAR CORRELATION FUNCTION

The effect of magnification bias due to weak gravitational lensing on the galaxy angular correlation function $\omega(\theta)$ has been derived in Villumsen (1996). Written in terms of the time-dependent power spectrum instead of the present day one, which makes it applicable to nonlinear power spectra, $\omega(\theta)$ is given by

$$\omega(\theta) = 4\pi^2 \int_0^{\chi_H} d\chi [W(\chi)a(\chi)b(\chi) + 15\Omega_m(s - 0.4)g(\chi)]^2 \times \int_0^\infty dk k \frac{P(\chi, k)}{a^2(\chi)} J_0[kr(\chi)\theta]. \quad (2)$$

In this section the physical meaning of the various terms in the above equation and the notation used will be clarified.

We have used the notation of Jain & Seljak (1997), where χ is the radial comoving distance, χ_H that to the horizon, $r(\chi)$ is the comoving angular diameter distance, $W(\chi)$ the normalized radial distribution of galaxies in the sample, and

$$g(\chi) = r(\chi) \int_\chi^{\chi_H} \frac{r(\chi' - \chi)}{r(\chi')} W(\chi') d\chi'. \quad (3)$$

From the expression for the unperturbed line element

$$ds^2 = a^2(\tau) (-d\tau^2 + d\chi^2 + r^2(d\theta^2 + \sin^2\theta d\phi^2)), \quad (4)$$

τ being conformal time, it follows that

$$r(\chi) = \sin_K \chi \equiv \begin{cases} K^{-1/2} \sin K^{1/2} \chi, & K > 0 \\ \chi, & K = 0 \\ (-K)^{-1/2} \sinh(-K)^{1/2} \chi, & K < 0 \end{cases} \quad (5)$$

where K is the spatial curvature. Note that for a delta-function distribution of galaxies, $W(\chi') = \delta(\chi' - \chi_s)$, $g(\chi)$ reduces to $g(\chi) = r(\chi)r(\chi_s - \chi)/r(\chi_s)$. This notation is related to the one of Villumsen (1996) through $\chi = x$, $r(\chi) = y(x)$, $W(\chi)/r^2(\chi) = S(x)$ and $g(\chi)/r(\chi) = w(x)$.

First we shall briefly describe the effect of magnification bias on $\omega(\theta)$. Gravitational lensing of a galaxy by dark matter concentrations between us and the galaxy increases the area of the galaxy image while conserving surface brightness. This results in a magnification μ which is given by the ratio of lensed to unlensed area of the image. The amplitude of μ depends on the convergence κ , which is the surface mass density divided by the critical density, and the shear γ through (Young 1981)

$$\mu = \frac{1}{(1 - \kappa)^2 - \gamma^2} \quad (6)$$

In the limit of weak lensing, $|\kappa|, |\gamma| \ll 1$, applicable to lensing by large-scale structure, the above expression reduces to

$$\mu = 1 + 2\kappa \quad (7)$$

This magnification has two effects. Since the lensed area is increased due to deflection of the light rays, the number density of galaxies decreases inversely proportional to

μ . There is a competing effect, however. In a flux limited survey, magnification brings some faint galaxies above the flux limit, which would not otherwise have been detectable, thus increasing the number density of galaxies. Which of the effects wins depends on the reservoir of faint galaxies available, which can be quantified by the slope s of the true number counts $N_0(m)$ for a magnitude limit m ,

$$s = \frac{d \log N_0(m)}{dm}. \quad (8)$$

The two effects change the galaxy numbers by (e.g. Broadhurst, Taylor & Peacock 1995)

$$N'(m) = N_0(m)\mu^{2.5s-1} \quad (9)$$

which reduces to

$$N'(m) = N_0(m) [1 + 5(s - 0.4)\kappa] \quad (10)$$

in the weak lensing limit. In addition, the number density of galaxies is changed by δn due to intrinsic clustering. Let \bar{n} denote the average number density of galaxies. At a given position in the sky $\hat{\phi}$, the number density is thus changed to

$$n(\hat{\phi}) = \bar{n} (1 + \delta n(\hat{\phi}) + 5(s - 0.4)\kappa(\hat{\phi})). \quad (11)$$

Now we further assume that galaxies trace the underlying dark matter distribution so that the 3-dimensional galaxy overdensity is,

$$\delta_g(\vec{x}) = b \delta(\vec{x}), \quad (12)$$

where $\delta(\vec{x})$ is the dark matter overdensity and the bias b is the proportionality factor. In this linear bias model, the perturbed, projected number density is given by (Villumsen 1996)

$$\delta n(\hat{\phi}) = b \int_0^{\chi_H} d\chi W(\chi) \delta(r(\chi) \hat{\phi}). \quad (13)$$

whereas the convergence κ is given by (Villumsen 1996)

$$\kappa(\hat{\phi}) = \frac{3}{2} \Omega_m \int_0^{\chi_H} d\chi g(\chi) \frac{\delta(r(\chi) \hat{\phi})}{a}. \quad (14)$$

The angular correlation function $\omega(\theta)$ as defined in equation 1 involves the expectation value $\langle n(\hat{\phi})n(\hat{\psi}) \rangle$. Since both δn due to intrinsic clustering, and κ are related to δ according to Eqs. 13 and 14, intrinsic dark matter correlations will induce correlations among galaxies. There are three distinct effects: correlations among the galaxies tracing correlated dark matter densities, described by $\langle \delta n(\hat{\phi})\delta n(\hat{\psi}) \rangle$; among background galaxies being lensed by correlated dark matter concentrations, described by $\langle \kappa(\hat{\phi})\kappa(\hat{\psi}) \rangle$; and finally among background galaxies and the foreground galaxies tracing the correlated dark matter concentrations, which are responsible for the lensing of the background galaxies, described by the term $\langle \delta n(\hat{\phi})\kappa(\hat{\psi}) \rangle$.

The expressions for $n(\hat{\phi})$, $\kappa(\hat{\phi})$ and $\delta n(\hat{\phi})$ from the above equations are inserted into Eq. 1. Expressing $\delta(\vec{x})$ in terms of its Fourier transform $\delta(\vec{k})$ and performing the ensemble average $\langle \delta(\vec{k})\delta(\vec{k}') \rangle$ then introduces the power spectrum $P(\chi, k)$. One finally obtains the result of Eq. 2 (Villumsen 1996) by evaluating the integrals, under the further assumption of $\theta \ll 1$, and using the plane-parallel approximation that only Fourier modes with wave vectors nearly perpendicular to the line of sight $\hat{\phi}$ contribute to the integral.

In the previous paragraphs we discussed the origin of the three terms in the angular correlation function, obtained by multiplying out the squared bracket in Eq. 2. We can write them schematically as,

$$\omega(\theta) = \omega_{gg}(\theta) + \omega_{gl}(\theta) + \omega_{ll}(\theta). \quad (15)$$

The third term $\omega_{ll}(\theta)$ is proportional to the correlation function $C_{pp}(\theta)$ of galaxy image ellipticities (Villumsen 1996),

$$\omega_{ll}(\theta) = (2.5s - 1)^2 C_{pp}(\theta), \quad (16)$$

The dependence of this term on Ω_m and Ω_Λ is discussed in detail in Jain & Seljak (1997) (see also Bernardeau et al. 1997; Kaiser 1996).

2.1 Dependence of $\omega(\theta)$ on cosmological parameters

With the assumption of constant linear bias, we can factor out the constants involving bias, s and Ω_m , and write $\omega(\theta)$ as

$$\begin{aligned} \omega(\theta) = & 4\pi^2 [b^2 \tilde{w}_{gg}(\theta) + 30b\Omega_m(s - 0.4)\tilde{w}_{gl}(\theta) \\ & + 225\Omega_m^2(s - 0.4)^2 \tilde{w}_{ll}(\theta)]. \end{aligned} \quad (17)$$

Besides the explicit Ω_m dependence, $\omega(\theta)$ depends on Ω_m and Ω_Λ mainly through the evolution of the power spectrum and the dependence of $r(\chi)$ on Ω_m and Ω_Λ .

In the linear regime the power spectrum depends on the linear growing mode of density perturbations $D(\chi)$ and the normalization σ_8 as,

$$P(\chi, k) \propto [\sigma_8 D(\chi)]^2. \quad (18)$$

The linear growing mode is well approximated by (Carroll, Press & Turner 1992)

$$\begin{aligned} D(\chi) = & \frac{5}{2} a \Omega(a) [\Omega(a)^{4/7} - \lambda(a) \\ & + (1 + \Omega(a)/2)(1 + \lambda(a)/70)]^{-1}, \end{aligned} \quad (19)$$

where we have defined, following Mo, Jing & Boerner (1997), the time dependent fractions of density in matter and vacuum energy, $\Omega(a)$ and $\lambda(a)$ in terms of the present-day values Ω_m and Ω_Λ ,

$$\Omega(a) = \frac{\Omega_m}{a + \Omega_m(1 - a) + \Omega_\Lambda(a^3 - a)} \quad (20)$$

and

$$\lambda(a) = \frac{a^3 \Omega_\Lambda}{a + \Omega_m(1 - a) + \Omega_\Lambda(a^3 - a)}. \quad (21)$$

The spatial geometry also differs in different models, leading to a dependence of the angular distance $r(\chi)$ on Ω_m and Ω_Λ according to Eq. 5. These effects are contained in the terms $\tilde{w}_{gg}(\theta)$, $\tilde{w}_{gl}(\theta)$ and $\tilde{w}_{ll}(\theta)$ in Eq. 17.

On small scales (high- k) the growth of the power spectrum is significantly affected by nonlinear gravitational clustering. The nonlinear power spectrum is obtained from the linear one through the fitting formulae of Jain, Mo & White (1995) for $\Omega_m = 1$, and from those of Peacock & Dodds (1996) for the open and Λ -dominated models. These fitting formulae are based on the idea of relating the nonlinear power spectrum at scale k to the linear power spectrum at a larger scale k_L , where the relation $k(k_L, a)$ depends on

the power spectrum itself (Hamilton et al. 1991). They have been calibrated from and tested extensively against N-body simulations. For the linear power spectrum we take a CDM-like spectrum (Bardeen et al. 1986) with shape parameter $\Gamma = 0.25$, which provides a reasonable fit to the observed galaxy power spectrum. With this choice of the linear power spectrum, we use the fitting formulae for the fully nonlinear power spectrum as a function of a and k to evaluate equation 2 for $\omega(\theta)$.

Having specified the shape of the mass power spectrum, we need to set the global cosmological parameters Ω_m and Ω_Λ . The normalization of the power spectrum in turn will depend on these parameters. The four different cosmological models we consider include: a flat universe with $\Omega_m = 1$, an open model with $\Omega_m = 0.3$, and a flat Λ -dominated model, with $\Omega_m = 0.3$ and $\Omega_\Lambda = 0.7$. These three models are normalized to cluster abundances, which give the approximate relation (White et al. 1993; Viana & Liddle 1996; Eke, Cole & Frenk 1996; Pen 1996):

$$\sigma_8 = 0.6 \Omega_m^{-0.6}. \quad (22)$$

(For $\Omega_m = 0.3$, we use $\sigma_8 = 1$, which is slightly lower than given by the above relation.) Our fourth model is a flat universe, $\Omega_m = 1$, with a higher normalization of $\sigma_8 = 1$.

3 RESULTS FOR $\omega(\theta)$ WITH CDM-LIKE POWER SPECTRA

While the cosmological model is specified above, the galaxy population still needs to be described in terms of its redshift distribution, the number count slope s and the bias parameter b . We model the redshift distribution of galaxies by

$$n(z) = \frac{\beta z^2}{z_0^3 \Gamma[3/\beta]} \exp(-(z/z_0)^\beta), \quad (23)$$

for $\beta = 2.5$, which agrees reasonably well with the redshift distribution estimated for the Hubble deep field from photometric redshifts (Mobasher et al., 1996). $W(\chi)$ is related to the redshift distribution by $W(\chi) = n(z)H(z)$, where the expressions for the Hubble constant $H(z)$ and the radial comoving distance $\chi(z)$ depend on the background cosmology. The mean redshift is given by

$$\langle z \rangle = \frac{\Gamma(4/\beta)}{\Gamma(3/\beta)} z_0. \quad (24)$$

For a flat model with $\Omega_m = 1$, we obtain the R magnitude limit corresponding to a given mean redshift by interpolation of a set of estimated values from Charlot (1996). In this section we consider red and blue galaxy populations, with number count slopes $s_r = 0.25$ and $s_b = 0.45$ respectively, and a fixed bias $b = 1/\sigma_8$ for both samples. In the next section we will consider the more realistic case of a relative bias for the different colour samples, since red galaxies are more strongly clustered.

Figure 1 shows $\omega(\theta)$ for the $\Omega_m = 1$, $\sigma_8 = 1$ model. The linear and nonlinear predictions, shown by the solid and dashed curve, are compared with a power law shape with slope $\gamma = 0.8$. These curves are for $s = 0.4$, for which the lensing term drops out, and therefore show the contribution of the clustering term to $\omega(\theta)$. The effect of nonlinear

evolution enhances $\omega(\theta)$ for $\theta < 4'$, while it slightly suppresses $\omega(\theta)$ for $4' < \theta < 20'$. On larger scales the linear and nonlinear curves coincide. It is interesting that the nonlinear $\omega(\theta)$ is much closer to the observed power law than the linear curve which reflects the curvature of the CDM power spectrum. At large angles, $\theta > 10'$ the $\omega(\theta)$ curve starts to deviate from the power law shape. For the open and Λ dominated models, the results are similar, with the nonlinear contribution being larger than the $\Omega_m = 1$ model.

In Fig. 2 we show how lensing affects $\omega(\theta)$ in the flat $\Omega_m = 1$ cosmological model, for three values of the number count slope $s = s_b = 0.45$, $s = s_r = 0.25$, and $s = 0.4$. The mean redshift is 1, corresponding to an R magnitude limit of about 24.5. The $s = 0.4$ curve represents the intrinsic clustering as in the previous figure. For $s_b > 0.4$, the amplitude of $\omega(\theta)$ is increased due to lensing, and for $s_r < 0.4$ it is decreased. Magnification bias hardly changes the shape of $\omega(\theta)$ since the three curves are nearly parallel to each other.

In Fig. 3 we show the dependence of $\omega(\theta)$ on mean redshift of the sample. The contribution due to intrinsic clustering is shown for the four cosmological models, i.e. setting $s = 0.4$. Three values of θ are shown, ranging from $\theta = 1'$, where nonlinear effects are important, to $\theta = 20'$ where nonlinear effects become unimportant. At $\theta = 1'$, the models with low Ω_m have higher amplitudes than the models with $\Omega_m = 1$. This is because in the former models the growth of perturbations is slowed down at late times; when normalizing to present-day cluster abundances, this implies a higher normalization at earlier times compared to the $\Omega_m = 1$ models. This in turn means that nonlinear effects become important earlier on, and lead to a greater effect of nonlinear clustering by today. At large mean redshifts, however, the amplitude for the Λ -model dips below the $\Omega_m = 1$, $\sigma_8 = 1$ model. Here a competing geometrical effect starts to come in: at a given redshift a physical volume element is larger if $\Lambda > 0$ than in the absence of a cosmological constant, and therefore the intrinsic clustering is decreased. For $\theta = 20'$, this geometrical effect in the Λ -model is more noticeable and starts to be seen at lower mean redshifts because competing nonlinear effects are unimportant.

In Fig. 4 we plot $\omega(\theta)$ as a function of mean redshift for three values of s , as in Fig. 2, and for all four cosmological models. For the $\Omega_m = 1$ models, we also give the R magnitude limits inferred from Charlot (1996) on the top axis of the plot, corresponding to the mean redshifts shown on the bottom axis. These values are given as an orientation only, since the relation between R magnitude and mean redshift is not exactly linear, and depends on the model of galaxy evolution used to derive it. We can understand these results better by looking at the three terms of $\omega(\theta)$ in Eqs. 15 and 17 separately. At low mean redshifts, the intrinsic clustering term ω_{gg} dominates, but it decreases with redshift. At low $\langle z \rangle$ the cross-term ω_{gl} is much smaller than the intrinsic term, but it is approximately constant with redshift; ω_{ll} is even smaller than the cross-term due to the small lensing depth at small mean redshift, but it increases with $\langle z \rangle$. As the mean redshift of the sample increases, ω_{gg} drops, and the cross-term starts to become noticeable. The cross-term contains the factor $\Omega_m(s - 0.4)$, so that for $(s - 0.4) > 0$, $\omega(\theta)$ is increased with respect to the intrinsic contribution due to lensing, and for $(s - 0.4) < 0$ it is decreased. Also, the redshift at which this happens is larger for smaller Ω_m

and $|s - 0.4|$. At still larger $\langle z \rangle$, ω_{ll} has increased sufficiently to become noticeable as well. Since $\omega_{ll} \sim \Omega_m^2(s - 0.4)^2$ is always positive, its effect goes in the same direction as that of the cross-term for $(s - 0.4) > 0$. But for $(s - 0.4) < 0$, its effect is in the opposite direction to that of the cross-term, so that the decrease due to ω_{gl} is partly compensated.

The flat model with the higher normalization $\sigma_8 = 1$ shows a stronger lensing signal than the one with the lower $\sigma_8 = 0.6$, because the bias factor $b = 1/\sigma_8$ is smaller, which increases the lensing contribution from the cross-term $\omega_{gl} \sim b$ relative to the intrinsic clustering term $\omega_{gg} \sim b^2$.

In the open or Λ -model, as compared to the flat model, the change in growth rate of perturbations and the spatial geometry affect the intrinsic clustering part of $\omega(\theta)$ as discussed above. The geometric effect for $\Lambda > 0$, which decreases the intrinsic clustering, is the opposite of the lensing part. Since the volume element is larger, the optical depth to lensing is larger, and lensing is more effective. This explains why the amplitudes for red and blue samples deviate more strongly than in the $\Omega_m = 1$ case in spite of the extra factor of Ω_m in front of the cross-term $\tilde{\omega}_{gl}$. For the open model also this geometric effect is present, and compensates for some of the decrease due to the Ω_m -prefactor, but it is weaker than in the Λ model.

4 COMPARISON OF RED AND BLUE SAMPLES

The results presented so far for $\omega(\theta)$ include the contribution from intrinsic clustering and from lensing. It is interesting to consider measurable statistics that are more sensitive to the lensing contribution; in this section we show that the ratio of $\omega(\theta)$ for red and blue samples is one such example. We assume the presence of a population of blue galaxies with a number count slope $s_b = 0.45$ out to $z \gtrsim 1$, and also of a population of red galaxies with a slope of $s_r = 0.25$. A sample with such a slope may be obtained by defining color selected subsamples (Villumsen et al. 1997), using the fact that the number count slope is a decreasing function of $V - I$ color (Broadhurst et al. 1997).

Since red and blue galaxy samples are observed to have a relative bias at present, with red galaxies being more strongly clustered (they are more likely to be found in the centers of clusters) than blue ones, in this section we consider a bias factor for the red sample b_r which is larger than the bias b_b of the blue sample. We assume the individual biases to be constant in time, and we neglect possible physical evolution of the spatial correlation function (besides the one due to gravitational evolution).

In the absence of lensing, and assuming one has selected samples with the same redshift distribution, the ratio of $\omega(\theta)$ of the blue and red samples would be equal to the ratio of their relative biases squared,

$$\frac{\omega(\theta; s_b)}{\omega(\theta; s_r)} = \left(\frac{b_b}{b_r}\right)^2. \quad (25)$$

However, lensing changes this relationship. In the regime where the cross-term dominates the third term, the lensing contribution increases $\omega(\theta)$ for the blue, and decreases it for the red sample.

In Fig. 5 we plot $(b_r/b_b)^2 \omega(\theta; s_b)/\omega(\theta; s_r)$, which ought

to be equal to 1 in the absence of lensing, versus mean redshift for $\theta = 1', 5', 20'$, and a relative bias of two of the red and blue samples. The four curves show the results for the different cosmological models considered (see Section 2). We can see that there is only little variation with angle as expected from the results of Fig. 2. For intermediate mean redshifts $\langle z \rangle \lesssim 1$ we can neglect the ω_{ll} -term, and expand in the small quantity $\tilde{\omega}_{gl}/\tilde{\omega}_{gg}$ to see the dependence on bias factors and number count slope,

$$\frac{\omega(\theta; s_b)}{\omega(\theta; s_r)} \approx \left(1 + 30\Omega_m \left[\frac{s_b - 0.4}{b_b} - \frac{s_r - 0.4}{b_r} \right] \frac{\tilde{w}_{gl}(\theta)}{\tilde{w}_{gg}(\theta)} \right) \times \left(\frac{b_b}{b_r} \right)^2. \quad (26)$$

For $\langle z \rangle \gtrsim 1.5$, ω_{ll} can no longer be neglected. As discussed in the previous section, this term has the effect of compensating some of the decrease in amplitude of $\omega(\theta)$ due to the cross-term for the red sample, and the exact redshift at which this happens depends on Ω_m and $(s - 0.4)$. This effect is responsible for the flattening off of the ratio seen in Fig. 5. At still larger redshifts, (not plotted here), the ratio would decrease again.

As discussed in Section 3, for the open and Λ -dominated models, both the growth rate of perturbations and the spatial geometry are different from the $\Omega_m = 1$ model. By taking the ratio of two correlation functions, the effect of the growth rate cancels out, so that we are left with the effect of the different geometries on the three terms. For the Λ -dominated model the geometrical effect is largest, so that in spite of the factor of Ω_m in the cross-term, the ratio is larger than for the flat model normalized to $\sigma_8 = 0.6$. It even attains a value comparable to the $\Omega_m = 1$ model with the higher normalization of $\sigma_8 = 1$. Recall that a larger σ_8 favors the lensing contribution over the intrinsic clustering since the bias factor $b = 1/\sigma_8$ is smaller, and $\omega_{gl} \sim b$ whereas $\omega_{gg} \sim b^2$. For the open model the geometrical effect is not as important, and the ratio is below that for the flat case.

5 CONCLUSIONS

We have quantified the effect of gravitational lensing by large-scale structure on the angular correlation function of galaxies $\omega(\theta)$, for different cosmological models, on angular scales ranging from $1'$ to $20'$. We have taken into account nonlinear gravitational clustering which affects both the intrinsic clustering and lensing contributions to $\omega(\theta)$.

We find that the ratio of the angular correlation function for red and blue galaxy samples, normalized by the inverse of the relative bias of the two samples, deviates from the value of 1 expected in the absence of lensing at sufficiently large mean redshifts of the sample. For a mean redshift of 1.3 of the sample, this ratio rises to about 1.5 for the model with $\Omega_m = 1$ and $\sigma_8 = 1$, and continues to rise, flattening off, until it reaches 1.7 by a mean redshift of 2. At $\langle z \rangle = 1.3$ it rises to about 1.3 for the model with $\Omega_m = 1$ and $\sigma_8 = 0.6$, and to about 1.2 for the open model. In the Λ -dominated model, the ratio reaches a value of about 1.4 at $\langle z \rangle = 1.3$, and continues to rise to a value of about 1.6 at a mean redshift of 2. These values are at $1'$ angular separation; for larger angles they differ somewhat, but not to a great extent as shown in Fig. 5. The largest uncertainty

in the application of this result is due to the assumption of two populations with different number count slopes but the same redshift distribution with $\langle z \rangle \gtrsim 1$.

The effect of magnification bias on the angular correlation function could be used in future surveys, such as the ESO imaging survey (Renzini et al. 1996), to detect weak lensing by large-scale structure and constrain the cosmological parameters Ω_m and Ω_Λ . The ESO imaging survey aims to detect about 200-300 galaxies with redshifts between 1 and 2.8 in a field of 25 arcminutes squared, and a similar number with redshifts larger than 2.8 in a field ten times larger. One problem with trying to detect the effect of magnification bias on $\omega(\theta)$ is that unknown physical evolution of the galaxies can modify the intrinsic clustering and introduce uncertainties which may be larger than the lensing signal. The presence of bias evolution would introduce further uncertainties. In future work, we plan to study the cross-correlation of two galaxy samples with different mean redshifts and non-overlapping redshift distributions (Moessner & Jain 1997). In this way we hope to minimize the importance of uncertainties due to intrinsic clustering and the exact form of the redshift distribution, and propose a measurable statistic that is dominated by the lensing contribution.

6 ACKNOWLEDGEMENTS

We would like to thank Matthias Bartelmann, Teresa Brainerd, Peter Schneider, Uroš Seljak and Simon White for useful discussions.

REFERENCES

- Bardeen, J. M., Bond, J. R., Kaiser, N., & Szalay, A. S., 1986, ApJ, 304, 15.
- Bernardeau, F., van Waerbeke, L., & Mellier, Y. 1997, A&A, 322, 1.
- Blandford, R., Saust, A., Brainerd, T., & Villumsen, J., 1991, MNRAS, 251, 600.
- Broadhurst, T., Taylor, A., Peacock, J. 1995, ApJ, 438, 49.
- Broadhurst, T., Villumsen, J., Smail, I., Charlot, S., 1997, in preparation.
- Carroll, J., Press, W., Turner, E., 1992, ARAA, 30, 499.
- Charlot, S., 1996, private communication.
- Eke, V. R., Cole, S., & Frenk, C. S. 1996, MNRAS, 282, 263.
- Hamilton, A. J. S., Kumar, P., Lu, E., & Matthews, A. 1991, ApJ, 374, L1.
- Jain, B., Mo, H., White, S. D. M., MNRAS, 276, L25.
- Jain, B., Seljak, U., 1997, ApJ, 484, 560.
- Kaiser, N. 1996, astro-ph/9610120.
- Mo, H., Jing, Y.-P., Börner, G., 1997, MNRAS, 286, 979.
- Mobasher, B., Rowan-Robinson, M., Georgakakis, A., & Eaton, N., 1996, MNRAS, 282, 7.
- Moessner, R., & Jain, B., 1997, preprint.
- Peacock, J., Dodds, S., 1996, MNRAS, 280, 19.
- Pen, U. 1996, astro-ph/9610147.
- Renzini, A., da Costa, L., Freudling, W., d'Odorico, S., Quinn, P., Spyromilio, J., Beletic, J., ESO Imaging Survey observing proposal, 1996, <http://www.eso.org/vlt/eis>.
- Viana, P. T. P., & Liddle, A. R., 1996, MNRAS, 281, 531.
- Villumsen, J., 1996, MNRAS, submitted.
- Villumsen, J., Freudling, W., & da Costa, L., ApJ, 1997, 481, 578.

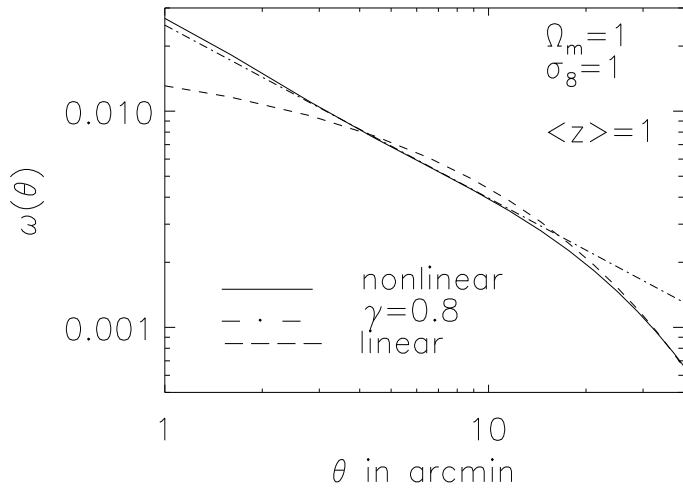


Figure 1. Angular correlation function as a function of angle for a mean redshift of 1, $\Omega_m = 1$, $\sigma_8 = 1$ and fixed bias $b = 1$. The slope of the number counts relation is $s = 0.4$. The dashed line shows the linear prediction, while the solid line is the nonlinear prediction. The nonlinear $\omega(\theta)$ is closer to the power law with slope -0.8 shown by the dash-dotted line.

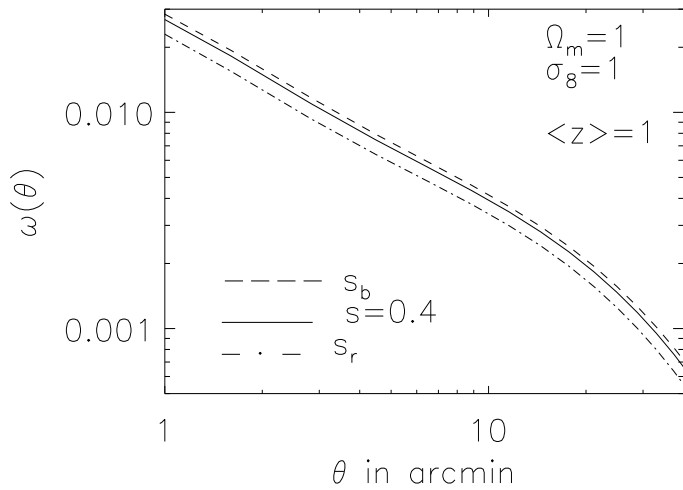


Figure 2. Angular correlation function as a function of angle for three values of the slope of the number counts relations: $s = 0.25, 0.4, 0.45$. As in Fig. 1, the mean redshift is 1, $\Omega_m = 1$, $\sigma_8 = 1$ and the bias is $b = 1$.

White, S. D. M., Efstathiou, G., & Frenk, C. S. 1993, MNRAS, 262, 1023.

Young, P., 1981, ApJ, 756.

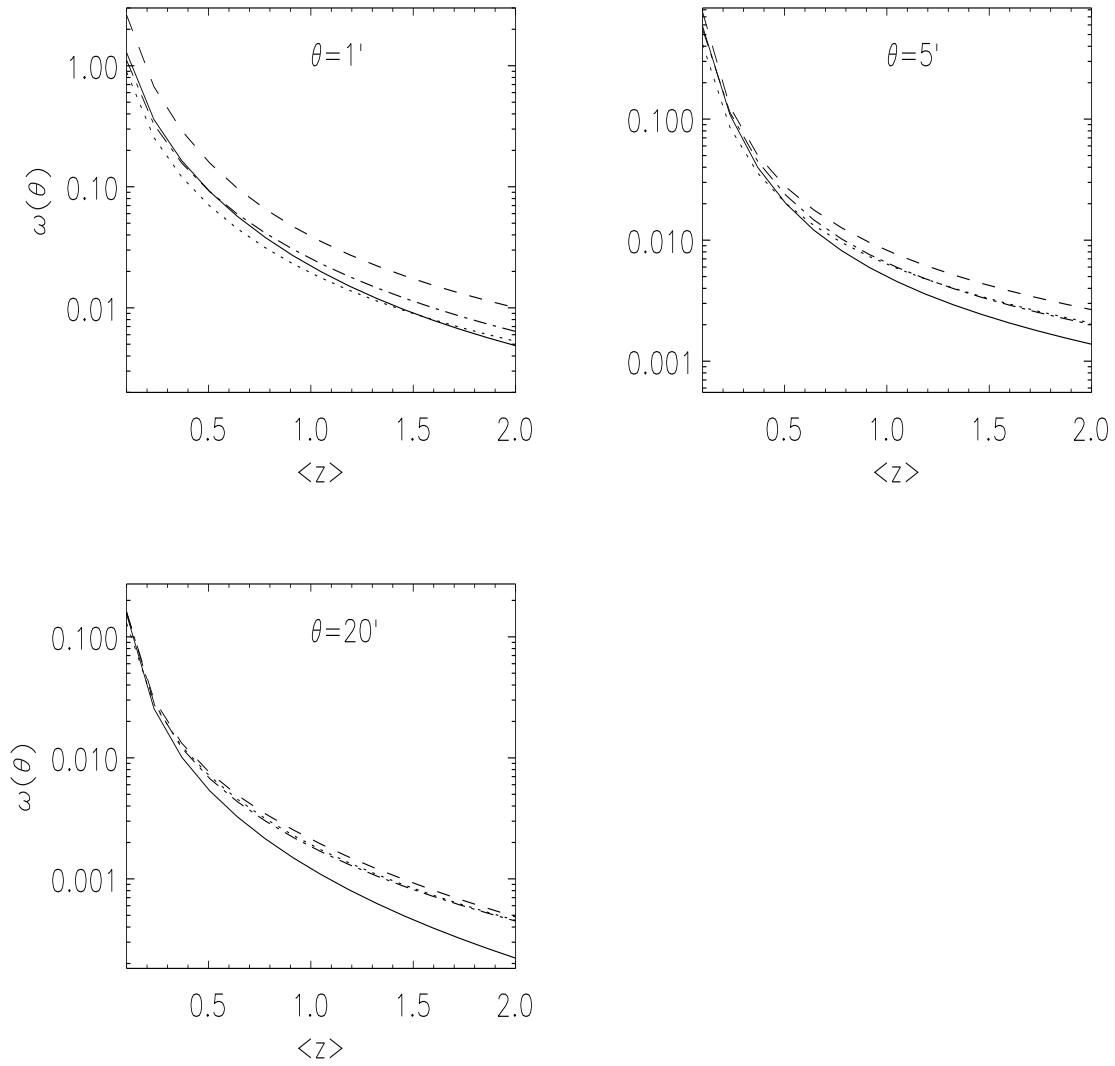


Figure 3. Comparison of angular correlation function due to intrinsic clustering ($s = 0.4$) for the four models, as a function of mean redshift of the sample. Plots for three angles are shown. The bias is fixed as $b = 1/\sigma_8$; the four models are: dash-dotted line: $\Omega_m = 1$, $\sigma_8 = 1$; dotted line: $\Omega_m = 1$, $\sigma_8 = 0.6$; dashed line: $\Omega_m = 0.3$, $\sigma_8 = 1$; solid line: $\Omega_m = 0.3$, $\Omega_\Lambda = 0.7$, $\sigma_8 = 1$.

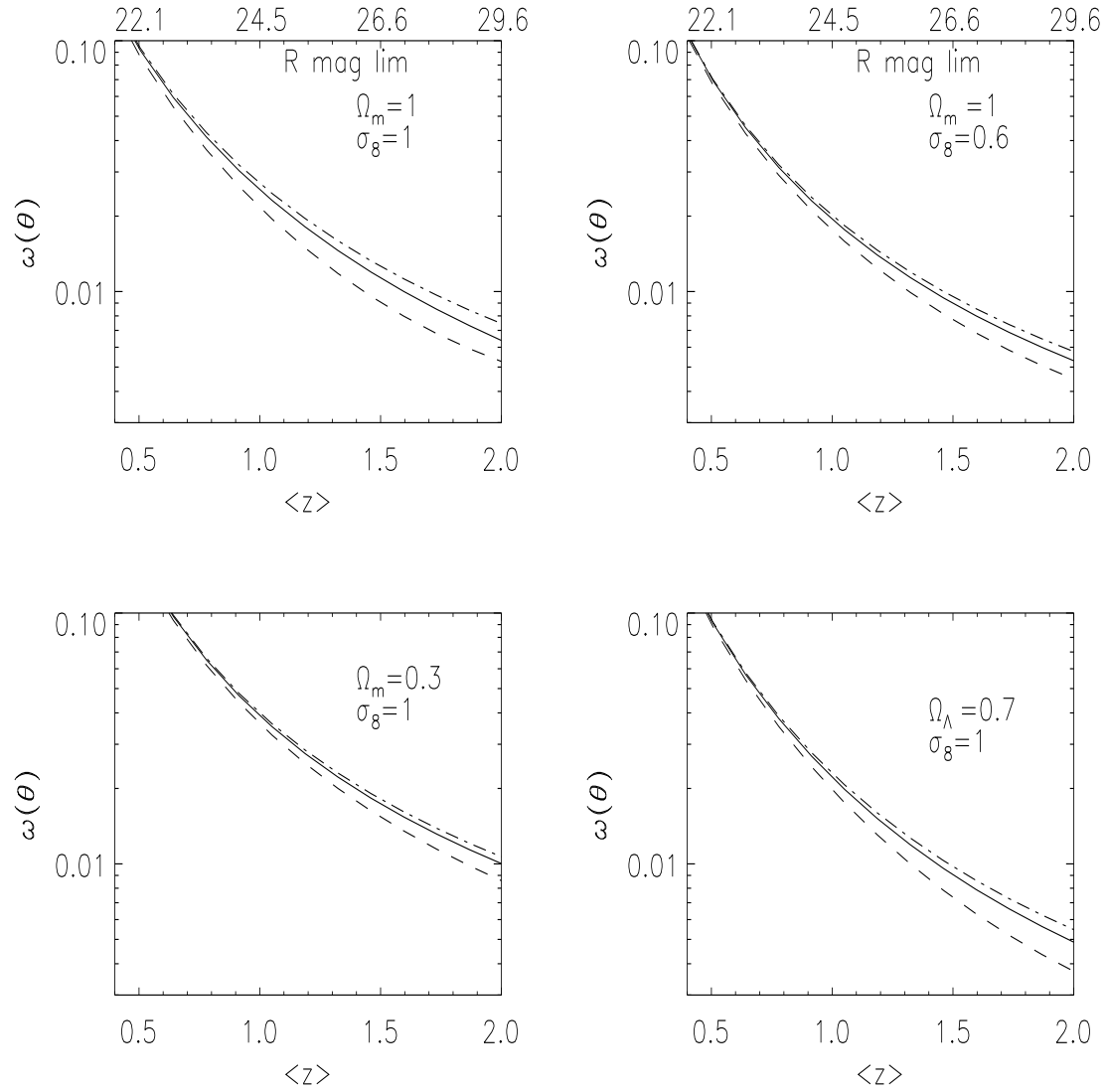


Figure 4. $\omega(\theta = 1')$ as a function of mean redshift for $s = s_b$ (dot-dashed line), $s = 0.4$ (solid line) and $s = s_r$ (dashed line). The bias is $b = 1/\sigma_8$, and the four cosmological models are as in Fig. 3. For the $\Omega_m = 1$ models we also indicate the corresponding limiting R magnitudes on the top axis.

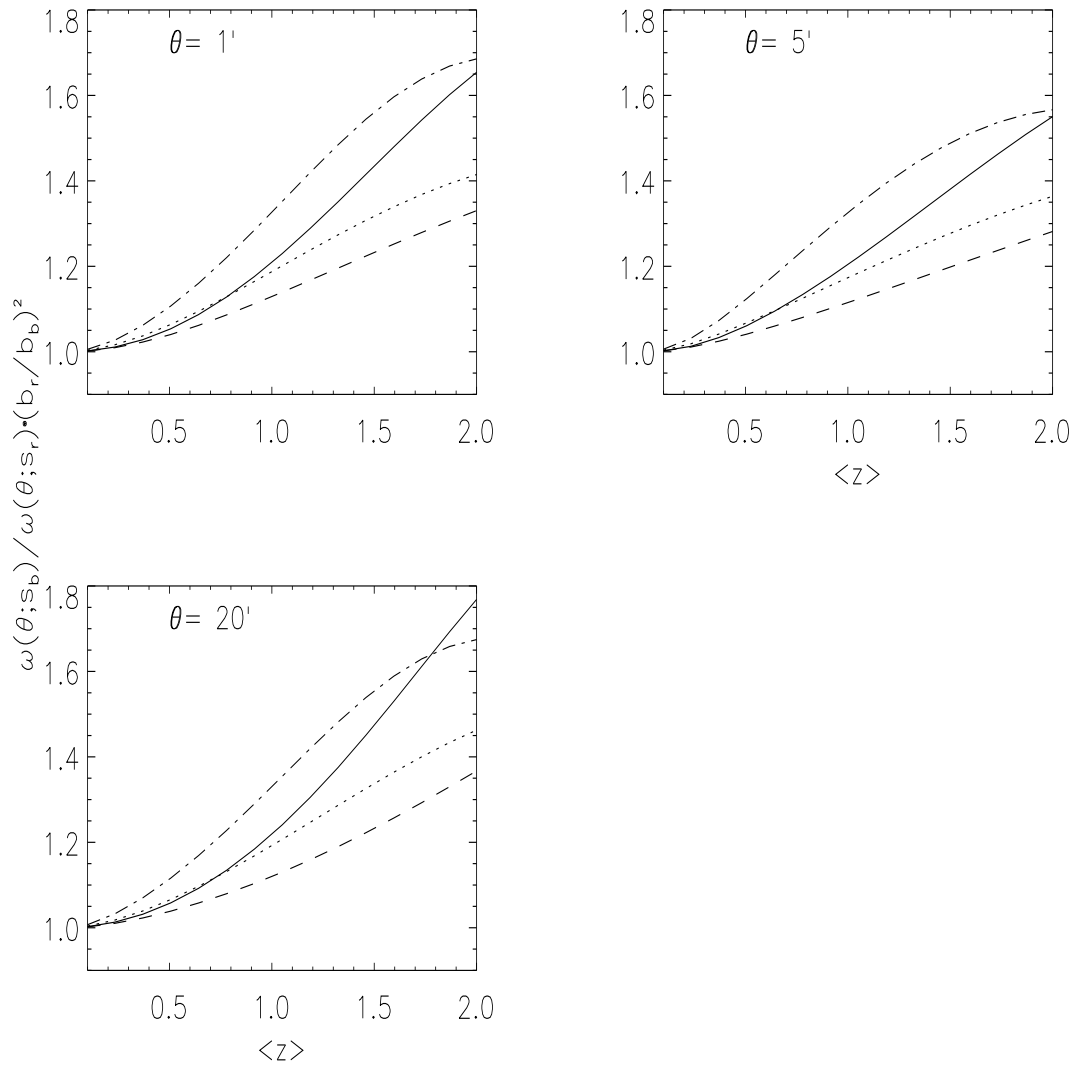


Figure 5. Ratio of $\omega(\theta)$ for red and blue samples times the inverse of the ratios of the bias factors squared ($b = 1/\sigma_8$, $b_r = b$, $b_b = b/2$). Dash-dotted line: $\Omega_m = 1$, $\sigma_8 = 1$; dotted line: $\Omega_m = 1$, $\sigma_8 = 0.6$; dashed line: $\Omega_m = 0.3$, $\sigma_8 = 1$; solid line: $\Omega_m = 0.3$, $\Omega_\Lambda = 0.7$, $\sigma_8 = 1$. Three values of θ are shown.